

See discussions, stats, and author profiles for this publication at: <https://www.researchgate.net/publication/264574894>

# Raman, Surface-Enhanced Raman, and DFT Characterization of (Diphenylphosphoryl) (pyridin-2-, -3-, and -4-yl)methanol

ARTICLE in THE JOURNAL OF PHYSICAL CHEMISTRY A · JULY 2014

Impact Factor: 2.69 · DOI: 10.1021/jp503392e

---

CITATION

1

READS

45

## 8 AUTHORS, INCLUDING:



[Edyta Proniewicz \(de domo Podstawka\)](#)

AGH University of Science and Technology in ...

98 PUBLICATIONS 1,135 CITATIONS

[SEE PROFILE](#)



[Ewa Pięta](#)

Jagiellonian University

14 PUBLICATIONS 13 CITATIONS

[SEE PROFILE](#)



[Bogdan Boduszek](#)

Wroclaw University of Technology

111 PUBLICATIONS 1,097 CITATIONS

[SEE PROFILE](#)



[Leonard M. Proniewicz](#)

Jagiellonian University

196 PUBLICATIONS 2,434 CITATIONS

[SEE PROFILE](#)

# Raman, Surface-Enhanced Raman, and Density Functional Theory Characterization of (Diphenylphosphoryl)(pyridin-2-, -3-, and -4-yl)methanol

Edyta Proniewicz,<sup>\*,†</sup> Ewa Pięta,<sup>‡</sup> Krzysztof Zborowski,<sup>‡</sup> Andrzej Kudelski,<sup>§</sup> Bogdan Boduszek,<sup>||</sup> Tomasz K. Olszewski,<sup>||</sup> Younkyoo Kim,<sup>⊥</sup> and Leonard M. Proniewicz<sup>‡</sup>

<sup>†</sup>Faculty of Foundry Engineering, AGH University of Science and Technology, ul. Reymonta 23, 30-059 Krakow, Poland

<sup>‡</sup>Faculty of Chemistry, Jagiellonian University, ul. Ingardena 3, 30-060 Krakow, Poland

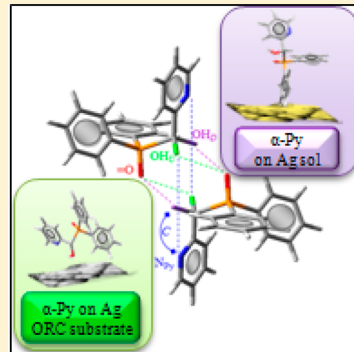
<sup>§</sup>Department of Chemistry, University of Warsaw, ul. L. Pasteura 1, 02-093, Warsaw, Poland

<sup>||</sup>Department of Organic Chemistry, Faculty of Chemistry, Wroclaw University of Technology, Wybrzeże Wyspiańskiego 27, 50-370 Wroclaw, Poland

<sup>⊥</sup>Department of Chemistry, Hankuk University of Foreign Studies, Yongin, Kyunggi-Do 449-791, Korea

## S Supporting Information

**ABSTRACT:** This work presents near-infrared Raman spectroscopy (FT-RS) and surface-enhanced Raman scattering (SERS) studies of three pyridine- $\alpha$ -hydroxymethyl biphenyl phosphine oxide isomers: (diphenylphosphoryl)(pyridin-2-yl)methanol ( $\alpha$ -Py), (diphenylphosphoryl)(pyridin-3-yl)methanol ( $\beta$ -Py), and (diphenylphosphoryl)(pyridin-4-yl)methanol ( $\gamma$ -Py) adsorbed onto colloidal and roughened in oxidation-reduction cycles silver surfaces. The molecular geometries in the equilibrium state and vibrational frequencies were calculated by density functional theory (DFT) at the B3LYP 6-311G(df,p) level of theory. The results imply that the most stable structure of the investigated molecules is a dimer created by two intermolecular hydrogen bonds between the H atom of the  $\alpha$ -hydroxyl group (in up ( $\text{HO}_U$ ) or down ( $\text{HO}_D$ ) stereo bonds position) and the O atom of tertiary phosphine oxide (=O) of the two monomers. Comparison the FT-RS spectra with the respective SERS spectra allowed us to predict the orientation of the hydroxyphosphonate derivatives of pyridine that depends upon both the position of the substituent relative to the ring N atom (in  $\alpha$ -,  $\beta$ -, and  $\gamma$ -position, respectively) and the type of silver substrate.



## INTRODUCTION

Organophosphorus compounds, utilized in the area of chemistry connected with medicine, agriculture, and industry, possess very interesting biological, chemical, and physical properties.<sup>1,2</sup> Among them,  $\alpha$ -hydroxy functionalized phosphonates and phosphine oxides are the most important. These molecules play a crucial role in inhibition of enzymes<sup>3,4</sup> and are potent agents in the treatment for bacterias,<sup>5,6</sup> viruses,<sup>7,8</sup> and tumors.<sup>9,10</sup> This is because these molecules are able to bind a metal.<sup>11</sup> For example, the hydroxyl group is a potent binding site at high pH. It was also found that the phosphine oxides containing pyridine (Py) are effective and highly stable bifunctional homogeneous metal complexes for oxidative catalysis and phase transfer reactions, which show hepatotoxic activity.<sup>12–14</sup> Metal complexes of  $\alpha$ -hydroxyphosphine oxides owe their stability to the basic lone pair of electrons on the N atom of pyridine. This lone pair of electrons does not belong to the pyridine  $\pi$ -electrons system. Thus, pyridine serves as a base that has chemical properties like those of tertiary amines. Additionally, at lower pH, the phosphinic oxygen may be also used as an another electron donor.

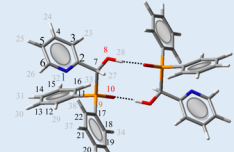
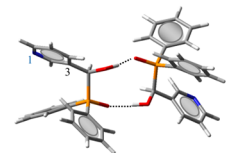
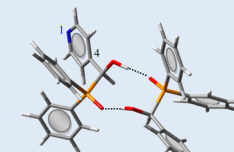
Although the biological significance of tertiary phosphine oxides containing both the pyridine and  $\alpha$ -hydroxy fragments is high, the data on this class of compounds are limited.<sup>15–17</sup> Thus, particular interest we placed on  $\alpha$ -,  $\beta$ -, and  $\gamma$ -isomers ( $\alpha$ ,  $\beta$ , and  $\gamma$  are positions of the substituent in respect to the N atom of Py) of pyridine- $\alpha$ -hydroxymethyl biphenyl phosphine oxide ( $\alpha$ -Py, (diphenylphosphoryl)(pyridin-2-yl)methanol;  $\beta$ -Py, (diphenylphosphoryl)(pyridin-3-yl)methanol;  $\gamma$ -Py, (diphenylphosphoryl)(pyridin-4-yl)methanol) (Table 1 presents molecular structures of the investigated compounds), performing vibrational spectroscopy studies on these molecules. We applied near-infrared Raman (FT-RS) and absorption infrared (FT-IR) spectroscopies that give the characteristic frequencies of the compounds and provide information on the structure of molecules over a broad range of physical states and temperatures.<sup>18–23</sup> To exactly and certainly explain the measured spectra, we extended our experiments by theoretical analysis using density functional theory (DFT) calculations at

Received: April 7, 2014

Revised: July 9, 2014

Published: July 10, 2014

**Table 1. Molecular Structure of the Pyridine- $\alpha$ -hydroxymethyl Biphenyl Phosphine Oxide Dimers with the Atom Numbering Scheme (According to the UPAC Nomenclature)**

molecular structure	abbreviation	name of monomer
	$\alpha$ -Py	(diphenylphosphoryl)(pyridine-2-yl)methanol
	$\beta$ -Py	(diphenylphosphoryl)(pyridine-3-yl)methanol
	$\gamma$ -Py	(diphenylphosphoryl)(pyridine-4-yl)methanol

Color legend:  – the carbon,  – the oxygen,  – the nitrogen,  – the phosphorus, and  – the hydrogen atoms

the B3LYP 6-311G(df,p) level of theory.<sup>24–26</sup> The B3LYP functional gives conformity of the theoretical vibrational spectra of organophosphonate compounds to the experimental data.<sup>27–30</sup>

The present study also involves the surface-enhanced Raman scattering (SERS) characterization of structure of the  $\alpha$ -,  $\beta$ -, and  $\gamma$ -isomers of pyridine- $\alpha$ -hydroxymethyl biphenyl phosphine oxide immobilized onto a colloidal and roughened in oxidation-reduction cycles (ORC) silver surfaces. The orientation of the surface species and a likely mode of their adsorption onto both substrates are proposed. This is because, unique information concerning the packing and geometry of molecules on metal can be obtained by using SERS. This information may have an important meaning in understanding of these compounds' *in vivo* behavior. SERS is a technique for examination of different kinds of supramolecular architectures and adsorption processes that occur at a metal/liquid interface.<sup>17,31,32</sup> On or close this interface molecules have fragments involved in the interaction with this interface. These moieties usually define the adsorbate geometry on the metal surface. Thus, analysis of the enhancement, broadness, and frequency of the SERS bands due to the molecular functional groups is crucial for describing a likely mode of the molecular interaction with the enclosing medium. However, this analysis is quite difficult and for correct interpretation so-called "surface selection rules", based on the electromagnetic mechanism of the SERS enhancement and on fact that adsorbate modes that involve changes in molecular polarizability with component normal to the surface are the strongest, should be considered.<sup>33,34</sup> For example, Creighton has demonstrated that the ratio of the surface enhancement factors for the  $A_2$ ,  $B_1$ , and  $B_2$  oscillations are 4:1:1 for a parallel aromatic molecule orientation and 1:1:4 for its perpendicular arrangement to the surface.<sup>35</sup> These quantities are bounded up with the symmetry

of the vibrations; the "out-of-plane" ( $A_2$ ) modes for the parallel orientation have a larger polarizability tensor component normal to the surface than the "in-plane" ( $B_2$ ) modes and *vice versa* for the vertical orientation.<sup>36</sup>

For the aromatic ring showing the  $C_{2v}$  point symmetry, assuming that the  $yz$  plane is the molecular plane and the  $z$  axis is the  $C_2$  axis of symmetry, the most enhanced SERS signals should transform as  $zz$  vibrations. Consequently, the next strong spectral features should transform as  $xz$  and  $yz$  vibrations. Thus, vibrations converting as  $xx$ ,  $xy$ , and  $yy$  should be negligibly enhanced or may not be observed at all. These rules together with the previously obtained results shown that the  $B_2$  modes transforming as  $yz$  should be pronounced at the time when the ring in-plane vibrational modes have a large component vertical to the metal surface. Therefore, on the one hand, in this position, the  $A_1$  converting as  $xx$ ,  $yy$ , and  $zz$ ,  $B_1$  transforming as  $xz$ , and  $\nu_2$  modes<sup>37</sup> are expected to be strong. On the other hand, vibrations of the  $A_2$  symmetry converting as  $xy$  should be absent due to the lack of  $z$  polarizability derivative component. In contrast, for the ring oriented horizontally, the  $A_2$ ,  $A_1$ , and  $B_1$  vibrations only should be strong. This selective enhancement results from the electromagnetic mechanism. However, Castro and co-workers have pointed out on lack of aromatic ring/metal interaction when there are both no prominent downshifts in frequency of the aromatic ring vibrations, mainly  $\nu_2$  and  $\nu_{12}$  modes, and no noticeable changes in the band widths.<sup>38</sup>

For N-containing heterocycles immobilized on metal surface, Carter and Pemberton have predicted two adsorption geometries,<sup>39</sup> i.e., flat-on and edge-on via the  $\pi$ -electrons system and N atom of Py, respectively. Generally, it can be said that for the flat-on geometry the frequency of the Py ring modes alter upon adsorption. For the edge-on geometry, the out-of-plane vibrations of Py are either absent or poorly scattered compared to the in-plane vibrations. Additionally, the ring breathing vibrations of adsorbed Py usually become stronger and frequencies for most of the bands shift down.

## EXPERIMENTAL AND THEORETICAL METHODS

**FT-RS Measurements.** The FT-RS spectra were measured on a Nicolet spectrometer, model NXR 9650, coupled with a continuum-wave Nd<sup>3+</sup>:YAG laser (1064 nm; the output laser power, 200 mW) and a liquid-nitrogen-cooled germanium detector. Usually, 1000 scans with a resolution of 4 cm<sup>-1</sup> were collected.

**SERS Measurements.** *Silver Sol.* AgNO<sub>3</sub> was purchased from Sigma-Aldrich (Poland) and used without further purification. Aqueous solution of the investigated compounds was prepared by dissolution of the proper compound in deionized water (18 MΩ cm). Briefly, 10 μL of 10<sup>-4</sup> M sample solution was mixed with a AgNO<sub>3</sub> solution. The formed silver-sample complex was irradiated by the 514.5 nm excitation line until the solution becomes yellow-brown, indicating the appearance of photoreduced colloidal nanoparticles. This observation was proved by the UV-vis spectrum and the TEM image (Figure 1). The TEM measurements clearly show the silver clusters with 15–20 nm in diameter and no identifiable form of the adsorbed compounds that randomly coat the metal substrate (Figure 1B).

The SERS spectra were collected three times from different spots using an InVia spectrometer (Renishaw). The spectral resolution was set at 4 cm<sup>-1</sup>. The diode laser was used as the

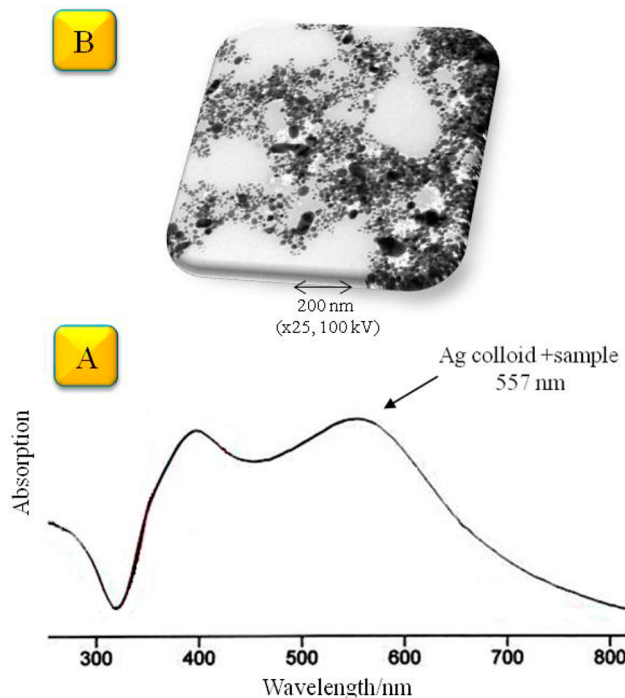


**Figure 1.** Excitation spectrum (UV-vis) (A) and transmission electron microscopy (TEM) image (B) of the sample/silver nanoparticles system.

excitation source (785.0 nm, the laser power at the sample: 10 mW).

**Roughened Silver Substrate.** The specially roughened in oxidation–reduction cycles (ORC substrate) silver substrates were prepared according to the standard procedure.<sup>40</sup> An overview of the morphology of this substrate (roughens size 50–150 nm) is given elsewhere.<sup>41</sup> The methodology of the SERS spectra measurements is described in ref 42.

**Transmission Electron Microscopy.** The TEM images of synthesized silver sol and sample/silver sol system were obtained by a transmission electron microscope (TEM) from Hitachi High-Technologies (model H-7650) at an accelerating voltage of 100 kV.

**Theoretical Analysis.** The Gaussian 03 software package (at the Academic Computer Center “Cyfronet” in Krakow) was

used to optimize the ground-state geometry of the pyridine- $\alpha$ -hydroxymethyl biphenyl phosphine oxide isomers as well as to model their experimental spectra.<sup>43</sup> The calculations were performed for monomers and various types of dimer species that are created by a pair of intermolecular hydrogen bonds between the H atom of the  $\alpha$ -hydroxyl group (in up ( $\text{HO}_U$ ) or down ( $\text{HO}_D$ ) stereo bonds position) and the O atom of tertiary phosphine oxide (=O) or the N atom of the pyridine ring ( $\text{N}_{\text{Py}}$ ) (in cis (C) or trans (T) position with respect to the  $\alpha$ -hydroxyl group;  $\text{HO}_C$  and  $\text{HO}_T$ , respectively) of the two monomers (see Table 2 for dimer description).

A DFT method with the B3LYP level of theory was applied to optimize the molecular structure of the investigated compounds. 6-311G(df,p), the split-valence triple- $\zeta$  basis set (6-311G), arising from the group of John Pople, supplemented by polarization functions, one set of d functions, and one set of f functions on heavy atoms as well as by one set of p functions on hydrogens, was used as the basis set.<sup>44,45</sup> No imaginary wavenumbers were calculated that prove that the optimized structures match to the energy minima on the potential energy surface for nuclear motion.

The calculated spectra (output files from the Gaussian) were inserted to the Raint program that allows us to calculate intensities for spectra measured at different excitation lines.<sup>46</sup> In our case we chose the 1064 nm line as an excitation wavelength, the same as we used in the experimental measurements. Then, the spectra were generated by the freeware GaussSum 0.8 software package (a scaling factor 0.981; a fwhm (full width at half-maximum) at 10  $\text{cm}^{-1}$ ; a 50%/50% Gaussian/Lorentzian band shape).<sup>47</sup> The PED (potential energy distribution) for monomers and dimers was determined with the freeware Gar2ped program<sup>48</sup> with implemented a specially written visualization script. The PED analysis in the high-frequency region for dimers was unsatisfying, due to the problems with defining of the eight-membered ring formed among two monomers in dimers; thus, PED for monomers is presented.

**Fitting Procedure.** The fitting procedure of the FT-RS and SERS spectra of the investigated pyridine- $\alpha$ -hydroxymethyl biphenyl phosphine oxides was performed with a GRAMS/AI program (Galactic Industries Co., Salem, NH).

**Table 2.** Various Types of Cyclic  $\alpha$ -,  $\beta$ -, and  $\gamma$ -Pyridine- $\alpha$ -hydroxymethyl Biphenyl Phosphine Oxide Dimers<sup>a</sup>

abbreviation			
$\alpha$ -Py dimers	$\beta$ -Py dimers	$\gamma$ -Py dimers	
=O···HO <sub>UC</sub>	=O···HO <sub>UC</sub>	=O···HO <sub>U</sub>	
=O···HO <sub>DC</sub>	=O···HO <sub>UT</sub>	=O···HO <sub>D</sub>	
=O···HO <sub>UT</sub>	=O···HO <sub>DT</sub>		
=O···HO <sub>DT</sub>	=O···HO <sub>DC</sub>		
N <sub>Py</sub> ···HO <sub>UC</sub>			
N <sub>Py</sub> ···HO <sub>DC</sub>			

Detailed description of the chemical structure diagram: The diagram shows two identical molecules of pyridine- $\alpha$ -hydroxymethyl biphenyl phosphine oxide. Each molecule has a pyridine ring with a phosphine oxide group (=O) at the 2-position and a biphenyl group at the 4-position. The biphenyl group has a hydroxymethyl group (-CH<sub>2</sub>OH) at the 4'-position. The molecules are oriented such that their α-hydroxyl groups (HO) are positioned to form a cyclic dimer. The HO groups are shown in green, and they are connected by dashed lines representing hydrogen bonds. The phosphine oxide groups are shown in orange, and the biphenyl rings are shown in grey. The diagram also indicates the C and T conformations of the hydroxyl groups relative to the pyridine ring and the U and D stereo positions of the hydroxyl groups.

<sup>a</sup>=O is the oxygen atom of the phosphine oxide. N<sub>Py</sub> is the N atom of Py. HO is the hydroxyl group. Subscripts C and T are the hydroxyl group in cis and trans conformations, respectively, with respect to N<sub>Py</sub>. Subscripts D and U are the hydroxyl group in down and up stereo bond positions, respectively.

**Table 3. Calculated Stabilization of the Energy for Monomers and Dimers of the Pyridine- $\alpha$ -hydroxymethyl Biphenyl Phosphine Oxide Isomers**

$\alpha$ -Py		$\beta$ -Py		$\gamma$ -Py	
dimer	stabilization energy [kcal/mol]	dimer	stabilization energy [kcal/mol]	dimer	stabilization energy [kcal/mol]
=O···HO <sub>UC</sub> dimer	17	=O···HO <sub>UC</sub> dimer	21	=O···HO <sub>U</sub> dimer	19
=O···HO <sub>UT</sub> dimer	21	=O···HO <sub>UT</sub> dimer	23	=O···HO <sub>D</sub> dimer	19
=O···HO <sub>DT</sub>	21	=O···HO <sub>DT</sub> dimer	22		
=O···HO <sub>DC</sub> dimer	12	=O···HO <sub>DC</sub> dimer	19		
N <sub>Py</sub> ···HO <sub>UC</sub> dimer	15				
N <sub>Py</sub> ···HO <sub>DC</sub> dimer	19				

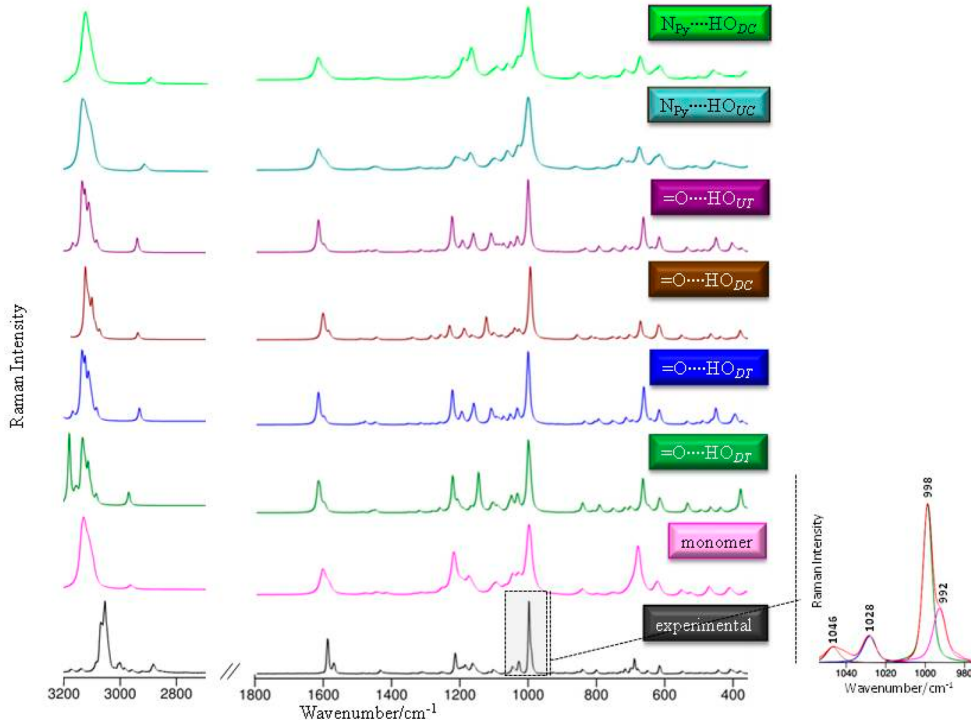


**Figure 2.** Experimental (black solid lines) and theoretical (colored lines) FT-RS spectra of monomer and various types of cyclic  $\alpha$ -Py dimers in the spectral ranges 3200–2750 and 1800–350  $\text{cm}^{-1}$ .

## RESULTS AND DISCUSSION

**Geometric Structures.** The calculated stabilization of the energy given in Table 3 indicates that the pyridine- $\alpha$ -hydroxymethyl diphenyl phosphine oxides monomers are less stable than dimers. Thus, monomers were not taken into consideration in further analysis. As is also evident from Table 3, the stabilization energy for =O···HO<sub>T</sub> dimers of  $\alpha$ -Py,  $\beta$ -Py, and  $\gamma$ -Py is higher than that for other dimers. Therefore, the =O···HO<sub>T</sub> dimers are the most stable. There are two possible conformers (U and D) of the dimers, depending on the positions of the H atom bonded to the O atom of the  $\alpha$ -hydroxyl group, whether they are directed up (HO<sub>U</sub>) or down (HO<sub>D</sub>) in the stereo bonds position (Table 2).

The =O···HO<sub>UT</sub> and =O···HO<sub>DT</sub> dimers have almost the same stabilization energy (Table 3). According to the Jeffrey system, the obtained results could be classified as *moderate* and *strong* hydrogen bonds.<sup>49</sup> Comparison of the =O···HO<sub>UT</sub> dimers theoretical spectra with the corresponding theoretical spectra of the =O···HO<sub>DT</sub> dimers points out the good similarity in the spectral patterns.

In addition, as is shown in Figures 2–4, for the =O···HO<sub>UT</sub> and =O···HO<sub>DT</sub> dimers theoretical Raman spectra are very much the same as the experimental Raman spectra of the  $\alpha$ -Py,  $\beta$ -Py, and  $\gamma$ -Py isomers. The N<sub>Py</sub>···H<sub>UC</sub> and N<sub>Py</sub>···H<sub>DC</sub> dimers were turned down on the basis of the Wu et al.<sup>50</sup> and Kiefer and co-workers<sup>51</sup> works that show that for the H-bonded pyridine nitrogen atom the spectral pattern, by means of wavenumbers and intensities of  $\nu_1$  and  $\nu_{12}$  modes, does not match the Raman spectral profile of the investigated  $\alpha$ -Py,  $\beta$ -Py, and  $\gamma$ -Py dimers.

The optimized equilibrium geometries, based on the DFT B3LYP 6-311G(df,p) level of theory, for the  $\alpha$ -,  $\beta$ -, and  $\gamma$ - (diphenylphosphoryl)(pyridin-2, -3, and -4-yl)methanol isomers structures are negligibly dependent on the formed H-bonds, in which the =O atom and  $\alpha$ -hydroxy group of the =O···HO<sub>DT</sub> and =O···HO<sub>UT</sub> dimers are involved. The hydrogen-bond distances are in the range 1.659–1.637 Å and are shorter than the P=O···H lengths in tertiary phosphine oxides (1.876–1.886 Å),<sup>52</sup> which is typical for carbonyl groups that are H-bonded to amines or alcohols. However, the value of 1.659–1.637 Å is very close to that observed for cavitand (1.5–1.6 Å).<sup>53</sup> The bond lengths and bond angles are listed in Table S1

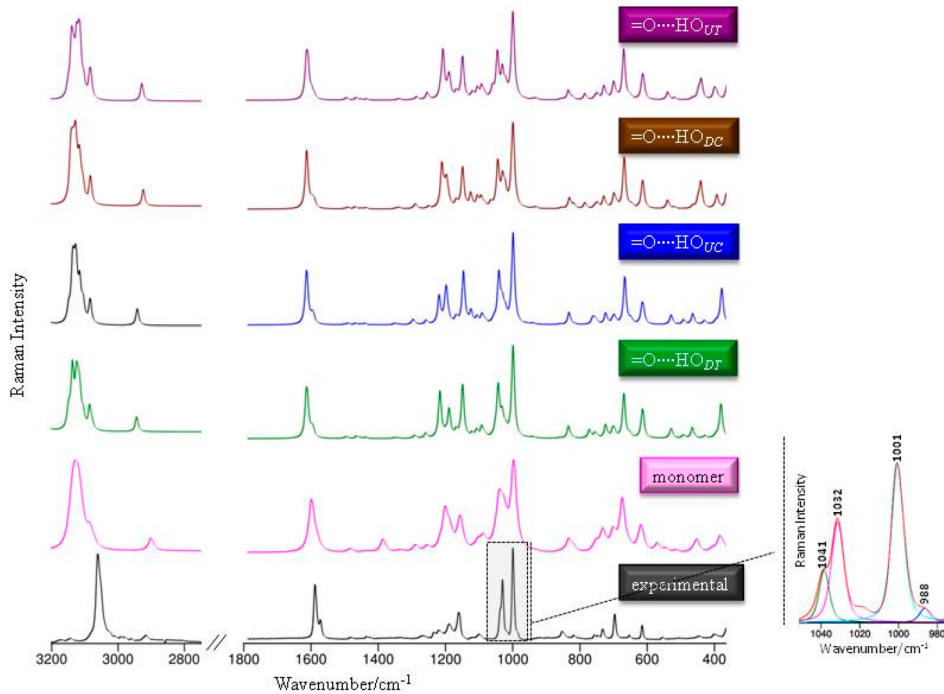


**Figure 3.** Experimental (black solid lines) and theoretical (colored lines) FT-RS spectra of monomer and various types of cyclic  $\beta$ -Py dimers in the spectral ranges 3200–2750 and 1800–350  $\text{cm}^{-1}$ .

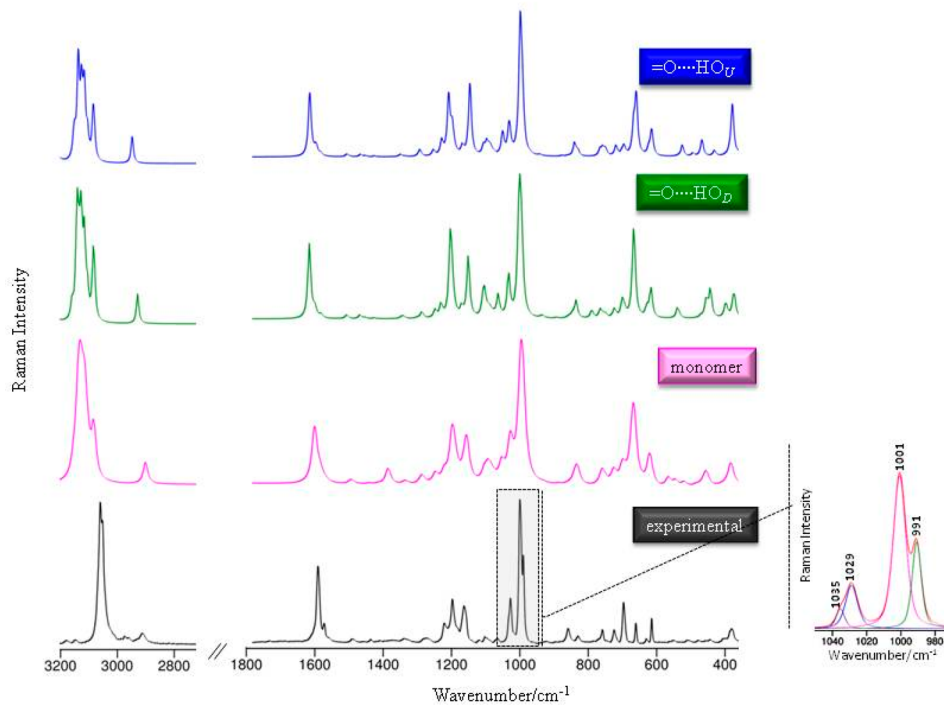


**Figure 4.** Experimental (black solid lines) and theoretical (colored lines) FT-RS spectra of monomer and various types of cyclic  $\gamma$ -Py dimers in the spectral ranges 3200–2750 and 1800–350  $\text{cm}^{-1}$ .

(Supporting Information, *Analysis of the molecular structures and the binding interaction*), whereas the atom numbering scheme for these molecules is given in Table 1.

**FT-RS and DFT Studies.** The experimental FT-RS spectra of three pyridine- $\alpha$ -hydroxymethyl biphenyl phosphine oxide isomers:  $\alpha$ -Py,  $\beta$ -Py, and  $\gamma$ -Py in the solid state together with corresponding theoretical spectra for the most stable dimers are

presented in Figure 5. Additionally, inset in Figure 5 shows the FT-RS spectrum of  $\alpha$ -Py in an aqueous solution. As is evident from Figure 5, there are no changes in the spectral profile between the spectra obtained for the  $\alpha$ -Py molecule in the solid state and in aqueous solution. This is in agreement with the previously published results<sup>41,54</sup> that proved that many compounds, including amino acids analogues, do not change

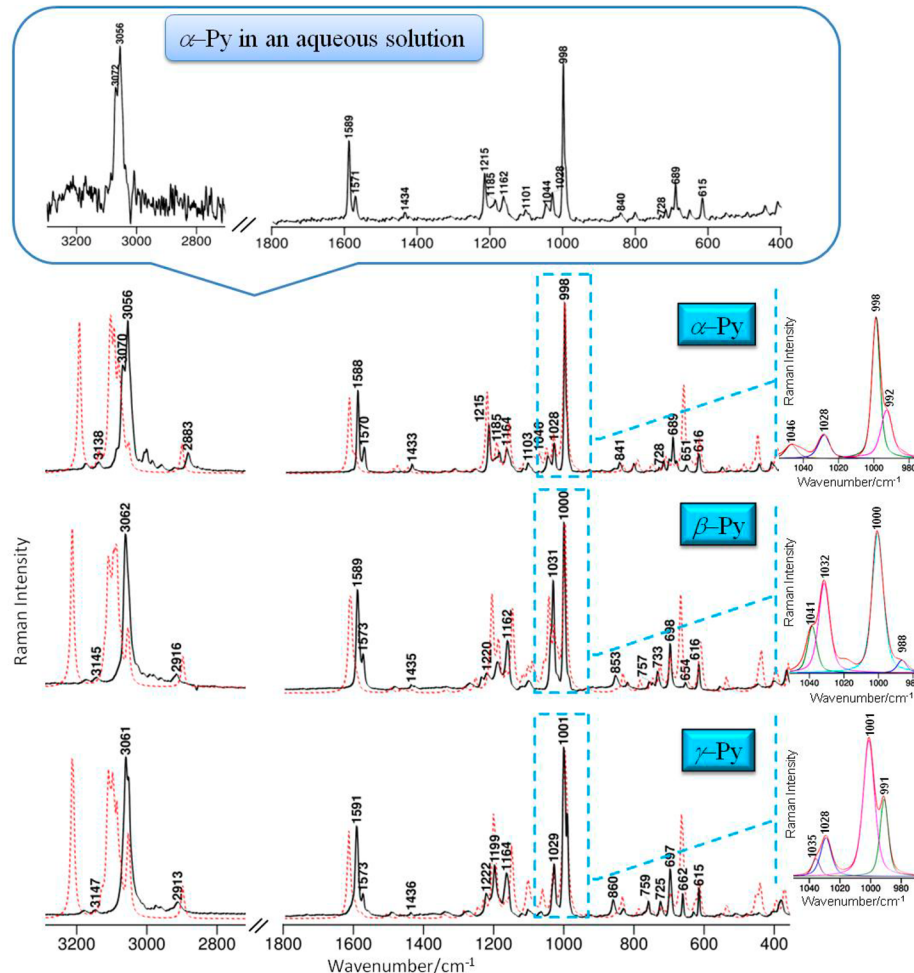


**Figure 5.** Experimental (black solid lines) and theoretical ( $=\text{O}\cdots\text{HO}_{\text{DT}}$ ,  $=\text{O}\cdots\text{HO}_{\text{UT}}$ , and  $=\text{O}\cdots\text{HO}_{\text{D}}$ , respectively) (red dashes lines) FT-RS spectra of  $\alpha$ -Py,  $\beta$ -Py, and  $\gamma$ -Py in the spectral ranges 3300–2750 and 1800–350  $\text{cm}^{-1}$ , and the FT-RS spectrum of  $\alpha$ -Py in aqueous solution (inset).

their molecular structures in going from the solid state to an aqueous solution, except at extreme pH conditions. Thus, we provided the FT-RS spectra of the investigated molecules in the solid state and compare these spectra with the respective SERS spectra.

The respective theoretical spectra for monomers and dimers (colored upper traces) are shown in Figures 2–4, in the spectral ranges 3200–2750 and 1800–350  $\text{cm}^{-1}$ . The measured FT-IR spectra with corresponding calculated spectra for the most stable dimers are shown in Figure S1 (Supporting Information). As is listed in Table S2 (Supporting Information), the calculated vibrational wavenumbers are very close to experimental ones. Table S2 (Supporting Information) gives also the potential energy distribution (PED, %) analysis.

In providing the definitive band assignment to the normal coordinates, literature dealing with isomeric phenyl-<sup>55–57</sup> and methylpyridines<sup>58</sup> and other related molecules, such as monosubstituted pyridines,<sup>47,59–61</sup> phenyls,<sup>36,38,62,63</sup> and phenylphosphine oxides,<sup>64</sup> have been considered together with the performed PED analysis (DFT, B3LYP 6-311G(df,p)) for the investigated  $\alpha$ -Py,  $\beta$ -Py, and  $\gamma$ -Py isomers (Table S2, Supporting Information). The modes due to the CC and CN bonds of the Ph and Py rings are mainly enhanced in the FT-RS spectra and are easily identified (Table S1, Supporting Information). Briefly, these modes exhibit comparable relative intensities among the isomers spectra and 16–19  $\text{cm}^{-1}$  splitting

(at 1588 and 1570  $\text{cm}^{-1}$  for  $\alpha$ -Py; at 1589 and 1573  $\text{cm}^{-1}$  for  $\beta$ -Py; at 1592 and 1573  $\text{cm}^{-1}$  for  $\gamma$ -Py). In the high-wavenumber range they show second overtones at  $\sim 3176$  ( $2 \times 1588 \text{ cm}^{-1}$ ) and  $\sim 3138 \text{ cm}^{-1}$  ( $2 \times 1570 \text{ cm}^{-1}$ ). Other vibrations assignable to Ph appear in the  $\alpha$ -Py FT-RS spectrum as the strong 998  $\text{cm}^{-1}$  band ( $\nu_{12}$ ; according to the Wilson numbering scheme<sup>65</sup>) and weak 1028  $\text{cm}^{-1}$  ( $\nu_{18}$ ) Raman signal (Table S1, Supporting Information). The relative enhancement of the aforementioned SERS signals changes for the remaining two isomers. The strength of the  $\nu_{12}$  mode remains almost unaltered among all the isomers' spectra but  $\nu_{18}$  considerably increases for  $\beta$ -Py. The corresponding breathing modes of the Py ring occur at around 988–992 ( $\nu_1$ ) and 1035–1046  $\text{cm}^{-1}$  ( $\nu_{12}$ ) and are much weaker than those for Ph, except for the  $\nu_1$  mode of  $\gamma$ -Py that shows half of the Ph  $\nu_{12}$  mode relative intensity. The  $\sim 654$  and  $\sim 616 \text{ cm}^{-1}$  Raman signals are also due to the Py and Ph ring stretching vibrations, respectively. The weak  $\sim 757$  and  $\sim 730 \text{ cm}^{-1}$  bands easily identified in the  $\beta$ -Py and  $\gamma$ -Py FT-RS spectra are assigned to triangular modes (in-plane CCC) of both aromatic rings. The in-plane CH bending ring modes are allocated as follows:  $\sim 1103$  (Py),  $\sim 1164$  (Ph),  $\sim 1185$  (Py), and  $1250$ – $1278$  (Py)  $\text{cm}^{-1}$ . However, the CH stretching vibrations are seen in the spectral range 3070–3056  $\text{cm}^{-1}$ . The medium  $\alpha$ -Py 1215  $\text{cm}^{-1}$  band that weakens in the  $\beta$ -Py and  $\gamma$ -Py FT-RS spectra is due to an X-sensitive vibration ( $\nu_{\text{CX}}$ ). However, this vibration does not exhibit splitting for the  $\alpha$ -Py

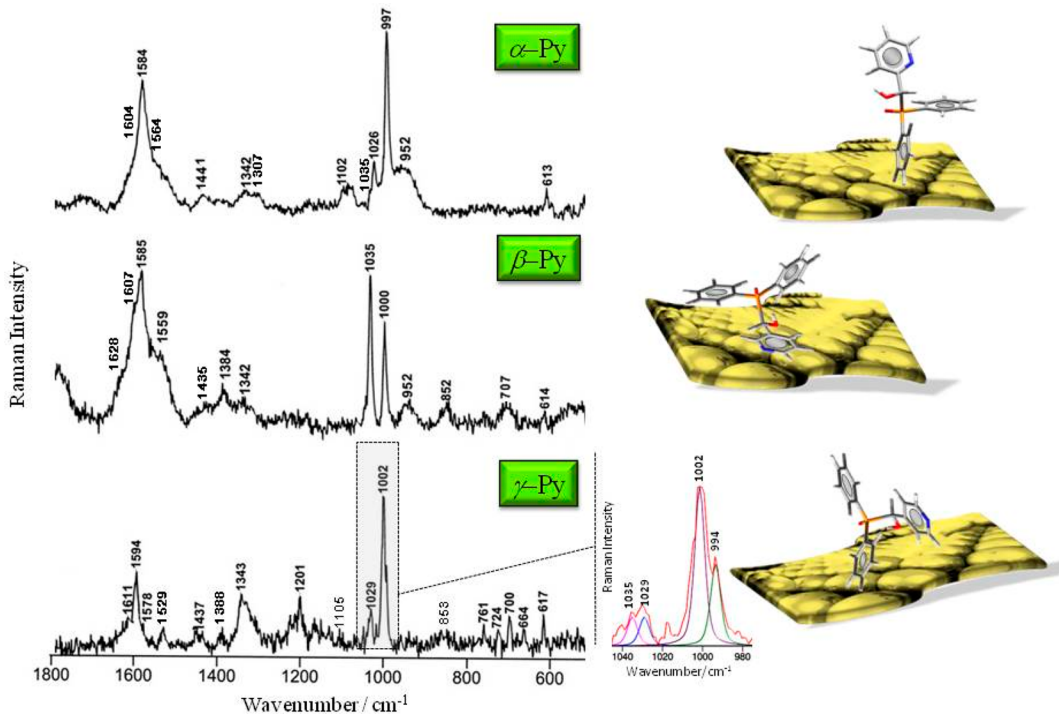


**Figure 6.** SERS spectra of  $\alpha$ -Py,  $\beta$ -Py, and  $\gamma$ -Py adsorbed onto a ORC substrate in the spectral range 1800–500  $\text{cm}^{-1}$ .

and  $\gamma$ -Py isomers, as in the case of  $\beta$ -Py. This mode shows two maxima at 1235 and 1220  $\text{cm}^{-1}$ . The weak  $\sim 841$  and  $\sim 813$   $\text{cm}^{-1}$  Raman signals are expected to derive from the out-of-plane CH wagging oscillations.

The  $\text{O}_8-\text{C}_7=\text{P}_9=\text{O}_{10}$  fragment vibrations do not affect the majority of the Py and Ph rings modes; however, the weak contributions could not be omitted. This can be seen at  $\sim 689$   $\text{cm}^{-1}$  in the  $\alpha$ -Py,  $\beta$ -Py, and  $\gamma$ -Py FT-RS spectra. The band at around this wavenumber is calculated to be the  $\text{P}_9-\text{C}_{\text{Ph}}$  stretch. The oscillations of the  $\text{P}_9-\text{C}_{\text{Ph}}$  bond also influence the Raman signals in the range between 700 and 730  $\text{cm}^{-1}$ , whereas the  $\text{C}_7-\text{C}_{\text{Py}}$  bond vibrations contribute to the 800–850  $\text{cm}^{-1}$  spectral features. In the case of  $\text{O}_8-\text{C}_7$  and  $\text{P}_9=\text{O}_{10}$ , it is expected that the stretching modes of these bonds appear at wavenumbers ranging from 1040 to 1220  $\text{cm}^{-1}$ . The detailed list of the  $\text{O}_8-\text{C}_7-\text{P}_9=\text{O}_{10}$  moiety vibrations is given in Table S2 (Supporting Information).

**SERS Studies. ORC Silver Substrate.** Figure 6 illustrates the SERS spectra of the investigated  $\alpha$ -,  $\beta$ -, and  $\gamma$ -pyridine- $\alpha$ -hydroxymethyl biphenyl phosphine oxide isomers immobilized onto the ORC silver substrate. As is apparent, the  $\alpha$ -Py SERS spectrum clearly possesses the characteristic Raman signals assigned to the Ph modes. However, in the SERS spectra of  $\beta$ -Py and  $\gamma$ -Py the spectral features due to Ph and Py are also detected. Table 4 summarizes the frequencies of these bands and their allocations to the normal mode motions (see Table S3 (Supporting Information) for the graphical representation of the vibrational modes).

According to the SERS studies for bis[(hydroxypyridin-3-yl)methyl]phosphinic acid deposited onto the ORC and colloidal silver substrates as well as for *o*-, *m*-, and *p*-pyridinecarboxylic acid in a silver sol,<sup>60</sup> the 707 ( $\rho_t(\text{Py})$ , of the  $\text{B}_1$  class symmetry mode), 1035 ( $\nu(\text{Py})_{\text{trig, breathing}, \text{A}_1}$ ), 1342 ( $\delta(\text{CH})_{\text{Py}, \text{B}_2}$ ), 1435 ( $\delta(\text{CH})_{\text{Py}, \text{B}_2}$ ), 1559 ( $\nu(\text{Py})_{\text{B}_2}$ ), 1585 ( $\nu(\text{Py})_{\text{A}_1}$ ), and 1628  $\text{cm}^{-1}$  ( $\nu(\text{Py})_{\text{A}_1} + (\delta(\text{Py}), \text{B}_2)$ ) SERS signals of  $\beta$ -Py are assigned to the Py vibrations. For these

modes, in general, the upshift in wavenumbers between the FT-RS and SERS spectra is observed ( $\Delta_\nu = 2$ –14  $\text{cm}^{-1}$ ). The 1035 and 1585  $\text{cm}^{-1}$  spectral features are the strongest in the spectrum, whereas the remaining spectral features are weak. In addition, the 1035  $\text{cm}^{-1}$  band shows a fwhm (9  $\text{cm}^{-1}$ ) similar to that in the  $\beta$ -Py FT-RS spectrum, but the 1585  $\text{cm}^{-1}$  band is broadened (fwhm = 51  $\text{cm}^{-1}$ ) and complex. This is due to the fact that, in this region, three aforementioned modes of Py overlap with two Ph CC vibrations. So, in the  $\beta$ -Py SERS spectrum, most of the  $\text{A}_1$  and  $\text{B}_2$  modes are enhanced. This fact points out that the pyridine ring of  $\beta$ -Py is horizontal to the ORC silver substrate.<sup>61</sup> The flat-on Py orientation allows the  $\text{C}_{\text{Py}}-\text{C}_7$  (at 852  $\text{cm}^{-1}$ ) and  $\text{C}_7-\text{O}_8-\text{H}_{28}$  (at 1384  $\text{cm}^{-1}$ ) moieties' oscillations to be enhanced as well as forces the Ph ring to adopt a tilted arrangement with respect to the ORC silver substrate, being in close proximity to it. This conclusion is mainly grounded on the 614 ( $\nu_{6b}$ ,  $\text{B}_2$ ), 952 ( $\nu_{5/17}$ ,  $\text{B}_1/\text{A}_2$ ), and 1000  $\text{cm}^{-1}$  ( $\nu_{12}$ ,  $\text{A}_1$ ) SERS signals. The 952  $\text{cm}^{-1}$  band is absent in the FT-RS spectrum, whereas the 1000  $\text{cm}^{-1}$  SERS signal weakens in comparison to the Raman enhancement and does not shift in wavenumber. The proposed orientation of  $\beta$ -Py on the ORC silver substrate is shown in Figure 6.

In the SERS spectrum of  $\alpha$ -Py deposited onto the ORC silver substrate, the above-mentioned set of three Ph bands (613 (very weak), 952, and 997  $\text{cm}^{-1}$ ) is also enhanced. In addition, the 1026  $\text{cm}^{-1}$  ( $\nu_{18}$ ) band is enhanced and the two Ph CC vibrations ( $\nu_{8a}$  and  $\nu_{8b}$ ) are clearly observed. These  $\nu_{8a}$  and  $\nu_{8b}$  overlapped bands are narrower than those in the  $\beta$ -Py spectrum, excluding probably the influence from Py. Neither a substantial downshift ( $\Delta_\nu = 6$   $\text{cm}^{-1}$ ) nor significant band broadening (Table 4) seen for the Ph modes in comparison to their frequency in the FT-RS spectrum suggests that the  $\pi$ -electrons' interaction of Ph with the the ORC silver surface is weak. This is because the Ph ring adopts the more or less perpendicular orientation to this surface that is in accordance with the propensity rules of the SERS electromagnetic

**Table 4.** Wavenumbers and Full Width at Half-Maximum of Selected Aromatic Ring Modes of the Pyridine- $\alpha$ -hydroxymethyl Biphenyl Phosphine Oxide Isomers<sup>a</sup>

mode	theoretical calculations		FT-Raman		Ag colloid		SERS	
	wavenumbers/cm <sup>-1</sup>	Raman activity [%]	$\nu/\text{cm}^{-1}$	fw hm/cm <sup>-1</sup>	$\nu/\text{cm}^{-1}$	fw hm/cm <sup>-1</sup>	$\nu/\text{cm}^{-1}$	fw hm/cm <sup>-1</sup>
$\alpha$ -Py								
$\nu_{6a}$ [ $\delta(\text{Ph})$ ]	622	3.2	616	7	616	8	613	7
$\nu_{6b}$ [ $\delta(\text{Py})$ ]	661	2.0	651	7				
$\nu_1$ [Py]	998	7.5	992	7				
$\nu_{12}$ [Ph]	1003	47.9	998	5	998	15	997	10
$\nu_{18}$ [Ph]	1029	15.8	1028	7	1028	16	1026	5
$\nu_{12}$ [Py]			1046	12			1035	8
$\nu_{19b}$ [ $\delta(\text{CH})_{\text{Py}}$ ]	1441	2.0	1433	8				
$\nu_{8b}$ [Py/Ph]	1584	8.6	1570	10	1590	21	1564	18
$\nu_{8a}$ [Py/Ph]	1585	22.6	1588	10	1601	9	1584	26
$\beta$ -Py								
$\nu_{6a}$ [ $\delta(\text{Ph})$ ]	622	5.0	616	6	617	9	614	4
$\nu_{6b}$ [ $\delta(\text{Py})$ ]	665	27.9	654	7	645	15		
$\nu_4$ [ $\rho_t(\text{Py})$ ]	698	2.4	698	8	701	11	707	23
$\nu_1$ [Py]	1000	8.3	988	8				
$\nu_{12}$ [Ph]	1002	64.9	1000	9	998	11	1000	8
$\nu_{18}$ [Ph]	1029	23.0	1031	9	1030	11		
$\nu_{12}$ [Py]	1042	43.6	1041	7	1045	12	1035	9
$\nu_{19b}$ [ $\delta(\text{CH})_{\text{Py}}$ ]	1440	0.9	1435	6	1435	23		
$\nu_{8b}$ [Py/Ph]	1579	10.2	1573	8	1587	20	1559	18
$\nu_{8a}$ [Py/Ph]	1586	51.3	1589	8	1600	12	1585	21
$\nu_1 + \nu_{6b}$ [Py]							1628	18
$\gamma$ -Py								
$\nu_{6a}$ [ $\delta(\text{Ph})$ ]	621	4.9	615	5	617	10	617	7
$\nu_{6b}$ [ $\delta(\text{Py})$ ]	667	21.4	662	5	648	27	664	7
$\nu_4$ [ $\rho_t(\text{Py})$ ]	702	5.0	697	9	694	18	700	7
$\nu_1$ [Py]			991	6			994	6
$\nu_{12}$ [Ph]	1002	59.5	1001	9	999	13	1002	11
$\nu_{18}$ [Ph]	1029	26.1	1028	10	1028	11	1029	10
$\nu_{12}$ [Py]			1035	6			1035	6
$\nu_{19b}$ [ $\delta(\text{CH})_{\text{Py}}$ ]	1440	0.9	1436	5	1437	32		
$\nu_{8b}$ [Py/Ph]	1583	8.1	1573	8	1588	21	1578	10
$\nu_{8a}$ [Py/Ph]	1586	31.2	1591	11	1600	12	1594	19
$\nu_1 + \nu_{6b}$ [Py]					1633	12		

<sup>a</sup>Abbreviations: Py, pyridine ring; Ph, phenyl ring;  $\nu$ , stretching;  $\delta$ , deformation;  $\rho_v$ , twisting vibrations.

mechanism (the strongest SERS bands is due to the  $\nu_{12}$  mode).<sup>27</sup> This is the case because the  $997\text{ cm}^{-1}$  band is the most prominent in the  $\alpha$ -Py SERS spectrum. The proposed orientation of  $\alpha$ -Py on the ORC silver substrate is shown in Figure 6.

The SERS signals due to Ph of  $\gamma$ -Py deposited onto the ORC silver surface agree with those discussed for  $\alpha$ -Py, in which Ph “stands” on the substrate ( $617$ ,  $1002$ ,  $1023$ ,  $1578$ , and  $1594\text{ cm}^{-1}$ ). However, important differences between the SERS spectra of  $\beta$ -Py and  $\gamma$ -Py are the disappearance of the formerly detected CC/CN modes ( $1595$ – $1560\text{ cm}^{-1}$ ), the large decrease in the relative intensity of the  $1035\text{ cm}^{-1}$  band, the appearance of the  $994\text{ cm}^{-1}$  SERS signal assigned to the totally symmetric ring breathing vibration, and the strengthening of the  $1343\text{ cm}^{-1}$  spectral feature. As is evident from Table 4, these SERS signals are due to the Py oscillations. Therefore, we suppose that the  $\gamma$ -Py isomer interacts with the ORC silver substrate also via Py. To propose the appropriate way of this interaction, the alternations in the enhancement, frequency, and width of these bands should be considered. For example, the  $1035$  and  $991\text{ cm}^{-1}$  SERS signals allocated to the trigonal and

totally symmetric modes of Py, respectively, negligibly shift in frequencies upon adsorption. Also, upon adsorption, their relative intensities and bandwidths do not change ( $\Delta_{\text{fwhm}} = \sim 3\text{ cm}^{-1}$ ). This tendency is seen not only for  $1035$  and  $991\text{ cm}^{-1}$  spectral features but, generally, for all the observed Py bands in the  $\gamma$ -Py SERS spectrum. The second mode from the doubly degenerated semicircle stretches, the  $\nu_{19b}$  mode ( $\sim 1437\text{ cm}^{-1}$ ), is also weak. It is worth mentioning that the  $\nu_{19b}$  mode with the  $B_2$  irreducible representation (the  $C_{2v}$  local symmetry point group) is expected at  $\sim 1440\text{ cm}^{-1}$  in the Py Raman spectra, whereas  $\nu_{19a}$  with the  $A_1$  irreducible representation should show up with strong intensity at around  $1480\text{ cm}^{-1}$ . In the presented SERS spectra a band at  $\sim 1440\text{ cm}^{-1}$  is closer to  $\nu_{19b}$  than to  $\nu_{19a}$  despite the intensity that can be very dependent upon the SERS effect. On the one hand, because the SERS calculations were not performed (too difficult and time-consuming at this stage of the project), the  $\sim 1440\text{ cm}^{-1}$  was assigned to this mode. On the other hand, because the  $\alpha$ ,  $\beta$ -, and  $\gamma$ -Py isomers spectra were compared, the given assignment does not change drastically the whole “picture” of adsorption discussed in the paper. It has to also be mentioned that these two modes are

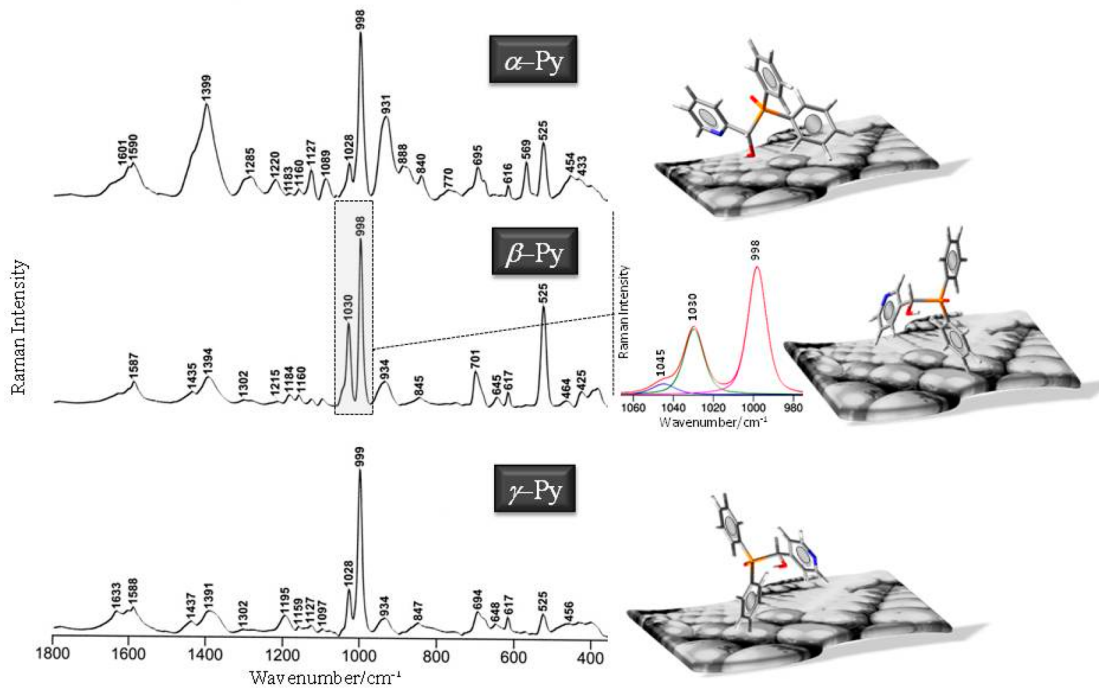


**Figure 7.** SERS spectra of  $\alpha$ -Py,  $\beta$ -Py, and  $\gamma$ -Py adsorbed onto a colloidal silver surface in the spectral range 1800–350  $\text{cm}^{-1}$ .

also assigned to  $\nu_{17}$  and  $\nu_5$ , respectively, by using different notations.<sup>66</sup>

On the basis of the above, the pyridine  $\pi$ -system weakly overlaps with this surface. In light of the above results, we suggest that Py of  $\gamma$ -Py adopts the perpendicular orientation onto the ORC silver substrate. In addition, the observed abrupt decrease in the relative intensity of the 853 ( $\text{C}_{\text{Py}}-\text{C}_7$  vibration) and 1388  $\text{cm}^{-1}$  ( $\text{C}_7-\text{O}_8-\text{H}_{28}$  moiety oscillations) spectral features, in comparison to those in the SERS spectrum of  $\beta$ -Py, implies that these molecular fragments are less involved in the interaction with the ORC silver surface for  $\gamma$ -Py than for  $\beta$ -Py. The proposed orientation of  $\gamma$ -Py on the ORC silver substrate is shown in Figure 6.

Although the electromagnetic mechanism plays an essential role in the enhancement of the Raman scattering, the contribution of the charge transfer (CT) mechanism to the enhancement for the investigated molecules deposited onto the ORC Ag substrate cannot be omitted. It has been noted that the CT mechanism contributes significantly to the relative intensities of the SERS bands of the benzene-like molecules, including pyridine.<sup>67</sup> This phenomenon is associated with enormous enhancement of the totally symmetric stretching ring mode ( $\sim 1600 \text{ cm}^{-1}$ ;  $\nu_{8a}$ ,  $A_1$ ), which is the most prominent band in the spectrum. The same results for methyl derivatives of pyridine and pyrazine have been achieved by Arenas et al.<sup>68</sup> Castro et al.,<sup>38</sup> studying phenylacetic acid and  $\alpha$ -phenylglycine immobilized onto silver substrates, have proposed a method that allows us to estimate the CT mechanism on the basis of the  $\nu_{8a}$  and  $\nu_{12}$  vibrations. The authors observed a significant decrease in the relative intensity of  $\nu_{12}$  and the enormous enhancement of the  $\nu_{8a}$  mode in the SERS spectra in comparison to the corresponding Raman spectra. This increase in  $I_{\nu_{8a}}$  they attributed to the CT mechanism of the enhancement. It is also worth mentioning that pyridine is the molecule with a low-lying unfilled  $\pi$ -orbital, which suggests that CT occurs from the metal surface to molecule.<sup>69</sup> Therefore, on

the basis of the strong enhancement of the Py  $\nu_{8a}$  and  $\nu_{12}$  modes, especially in the case of the  $\beta$ -Py compound, the CT mechanism plays an essential role in the adsorption process onto the ORC substrate.

**Colloidal Silver Substrate.** Noticeable spectral changes exist among the  $\alpha$ -Py,  $\beta$ -Py, and  $\gamma$ -Py isomers immobilized onto the ORC (Figure 6) and colloidal silver surfaces (Figure 7). In general, the ORC spectra are weaker and reflect less closely aromatic ring association with the surface than those measured for compounds in the presence of the silver sol. For instance, the well-defined bands near 1601, 1590, 1220, 1160, 1089, 1028, 998, and 616  $\text{cm}^{-1}$  in the  $\alpha$ -Py,  $\beta$ -Py, and  $\gamma$ -Py SERS spectra in the silver sol that correspond to those of Ph observed in the FT-RS spectra practically do not shift in wavenumbers and are in some cases negligibly broadened ( $\Delta_{\text{fwhm}} = 1-4, 11-13, 2-15, 1-5, 1-3, 1-9, 2-10$ , and  $1-5 \text{ cm}^{-1}$ , respectively) in comparison to their frequencies and widths in the FT-RS spectra (Table 4). Considering this, as well as the fact that the relative intensity ratio of these bands alters only slightly, except that of  $I_{\nu_{8a}}$ , which considerably decreases in the SERS spectra for molecules adsorbed onto silver nanoparticles, the nearly vertical arrangement of Ph to the colloidal silver nanoparticles surface is assumed for all the isomers.

Other direct evidence for interaction between Ph and the colloidal silver surface comes from the appearance of the  $\sim 931$  ( $\delta_{\text{oop}}(\text{CC}(\text{H})\text{C})$ ) and 695  $\text{cm}^{-1}$  ( $\nu(\text{P}_9-\text{C}_{\text{Ph}})$ ) bands. The former SERS signal is stronger for the  $\alpha$ -Py isomer than for  $\beta$ -Py and  $\gamma$ -Py, whereas the strength of the latter mode almost does not change among the isomers spectra. As a consequence of the  $\nu(\text{P}_9-\text{C}_{\text{Ph}})$  enhancement, the two new bands appear. First, a relatively narrow ( $\text{FWHM} = 16 \text{ cm}^{-1}$ )  $\sim 1127 \text{ cm}^{-1}$  spectral feature appears, medium intensity for  $\alpha$ -Py and weak for  $\beta$ -Py and  $\gamma$ -Py and characteristic of the  $\text{P}_9-\text{C}_{\text{Ph}}$  stretching vibrations. Second, a band located at 525  $\text{cm}^{-1}$  that involves oscillations of the molecular fragment consisting of the  $\text{P}_9$  atom (CCP, CPO, and PCO) is seen. In the case of  $\beta$ -Py, the 525

$\text{cm}^{-1}$  SERS signal is pronounced and decreases in the order  $\beta\text{-Py} > \alpha\text{-Py} > \gamma\text{-Py}$ . This may indicate some preference for the  $\text{C}_{\text{Py}}-\text{C}_7-\text{P}_9$  linkage of  $\beta\text{-Py}$  to be in close proximity to the colloidal silver surface. The  $1045 \text{ cm}^{-1}$  spectral feature due to the Py trigonal ring breathing observed only for  $\beta\text{-Py}$  may support this statement. However, several other the Py modes, i.e.,  $\sim 1633$ ,  $\sim 1183$ ,  $\sim 840$ , and  $\sim 644 \text{ cm}^{-1}$ , can be found in all the isomers' SERS spectra. These data point out that the pyridine ring of  $\beta\text{-Py}$  in a somehow tilted orientation occurs closer to the silver nanoparticles surface than that of the  $\alpha\text{-Py}$  and  $\gamma\text{-Py}$  isomers, in which case the ring seems to be more-or-less vertical.

Another interesting observation is the strengthening of the  $1399 (\text{C}_7-\text{O}_8-\text{H}_{28} \text{ deformation})$  and  $931 \text{ cm}^{-1}$  bands and the appearance of the  $569 \text{ cm}^{-1} (\gamma(\text{C}_7-\text{O}_8))$  SERS signal in the  $\alpha\text{-Py}$  spectrum. These phenomena together with the stronger enhancement of the  $1127 \text{ cm}^{-1}$  spectral feature (see discussion above) may suggest that the  $\text{C}_7-\text{O}_8$  molecular fragment of  $\alpha\text{-Py}$  is involved in the chemical interaction with the ORC substrate. Conversely, in  $\beta\text{-Py}$  and  $\gamma\text{-Py}$ , this moiety is in proximity to the colloidal silver surface.

## CONCLUSIONS

This work presents FT-RS and FT-IR spectroscopic studies, based on calculated frequencies and PED's, of the  $\alpha$ -,  $\beta$ -, and  $\gamma$ -pyridine- $\alpha$ -hydroxymethyl biphenyl phosphine oxide isomers. The molecular geometries in the equilibrium states and vibrational frequencies were calculated by density functional theory (DFT) at the B3LYP 6-311G(df,p) level using Gaussian'03, GaussSum 0.8, and GAR2PED softwares. Briefly, the performed investigations imply that the most stable structure of the investigated isomers is a dimer created by a pair of intermolecular hydrogen bonds between the H atom of the  $\alpha$ -hydroxyl group (in up ( $\text{HO}_U$ ) or down ( $\text{HO}_D$ ) stereo bonds position) and the O atom of tertiary phosphine oxide ( $=\text{O}$ ) of the two monomers. Therefore, the theoretical spectra and geometry parameters are given for dimers. For the dimers, there are two possible conformers (C and T) depending on the positions of the H atom bonded to the O atom of the  $\alpha$ -hydroxyl group, whether they are on the same ( $\text{HO}_C$ ) or opposite ( $\text{HO}_T$ ) side of the pyridine nitrogen atom.

This work also shows the results of the SERS investigations for the isomers immobilized onto the ORC (50–150 nm roughens size) and colloidal (15–20 nm particle size) silver substrates. On the basis of the SERS spectral profile, the adsorption modes of the  $\alpha\text{-Py}$ ,  $\beta\text{-Py}$ , and  $\gamma\text{-Py}$  isomers were suggested. The substituent position in the pyridine ring has an impact on the isomers geometry on the ORC substrate. However, this effect is weaker for molecules in the silver sol. Leaning on afore-discussed results and surface selection rules, it is obvious that the differences among the SERS spectra of the investigated isomers immobilized onto the two different silver SERS-active substrates are due to the differences in the molecular orientation, which depends on the surface roughness.

We demonstrated that on the ORC silver surface the phenyl ring of the  $\alpha\text{-Py}$  and  $\gamma\text{-Py}$  molecules adopt a perpendicular arrangement with respect to the metal surface, whereas for the  $\beta\text{-Py}$  this molecular fragment accepts the tilted orientation. In addition, the pyridine ring of  $\beta\text{-Py}$ , being in close proximity to this surface, is lying on the ORC substrate. However, Py in  $\gamma\text{-Py}$  is oriented vertically and is less involved in the interaction with the ORC substrate than in the case of  $\beta\text{-Py}$ .

On the one hand, in the case of the colloidal silver substrate, the Ph ring of all the pyridine- $\alpha$ -hydroxymethyl biphenyl phosphine oxide isomers is more or less vertical with respect to the silver nanoparticle surface and interacts with this substrate. On the other hand, the Py ring of  $\beta\text{-Py}$  adopts a tilted arrangement and is much closer to the surface than in the cases of  $\alpha\text{-Py}$  and  $\gamma\text{-Py}$  molecules, in which it seems to be more or less perpendicular.

## ASSOCIATED CONTENT

### S Supporting Information

(Diphenylphosphoryl)(pyridin-2-, -3-, and -4-yl)methanol synthesis. Geometric structures and geometry optimization. Experimental and theoretical FT-IR spectra of the investigated pyridine- $\alpha$ -hydroxymethyl biphenyl phosphine oxide isomers in the spectral range  $3500$ – $350 \text{ cm}^{-1}$ . Calculated bond lengths and angles of the pyridine- $\alpha$ -hydroxymethyl biphenyl phosphine oxide isomers. Calculated wavenumbers and potential energy distribution for the FT-RS and FT-IR spectra of the pyridine- $\alpha$ -hydroxymethyl biphenyl phosphine oxide isomers. The graphical representation of vibrational modes given in Table 4. This material is available free of charge via the Internet at <http://pubs.acs.org>

## AUTHOR INFORMATION

### Corresponding Author

\*E. Proniewicz. E-mail: proniewi@agh.edu.pl. Phone: +48-12-617-34-96. Fax: +48-12-633-6348.

### Notes

The authors declare no competing financial interest.

## ACKNOWLEDGMENTS

The authors are grateful to the Academic Computer Center "Cyfronet" in Krakow for the opportunity to carry out calculations. This work was supported by the Polish National Science Center (Grant No. N N204 544339 to E. Proniewicz). Y. Kim gratefully acknowledges HUFS for financial support.

## REFERENCES

- Olszewski, T. K. Environmentally Benign Syntheses of  $\alpha$ -Substituted Phosphonates: Preparation of  $\alpha$ -Amino and  $\alpha$ -Hydroxyphosphonates in Water, in Ionic Liquids, and Under Solvent-Free Conditions. *Synthesis* **2014**, *46*, 0403–0429.
- Naydenova, E. D.; Todorov, P. T.; Troev, K. D. Recent Synthesis of Aminophosphonic Acids as Potential Biological Importance. *Amino Acids* **2010**, *38*, 23–30.
- Stella, V. J.; Borchardt, R. T.; Hageman, M. J.; Oliyai, R.; Maag, H.; Tilley, J. W. *Prodrugs: Challenges and Rewards*; AAPS Press: New York, 2007.
- Demmer, Ch. S.; Krogsgaard-Larsen, N.; Bunch, Lennart. Review on Modern Advances of Chemical Methods for the Introduction of a Phosphonic Acid. *Chem. Rev.* **2011**, *111*, 7981–8006.
- Olszewski, T. K.; Boduszek, B. Application of Bis(trimethylsilyl) Phosphonite in the Efficient Preparation of New Heterocyclic -Aminomethyl- H -Phosphinic Acids. *Synthesis* **2011**, *3*, 0437–0442.
- Olszewski, T. K.; Boduszek, B. Synthesis of New Thiazole-2, -4, and -5-yl-(amino)methylphosphonates and Phosphinates: Unprecedented Cleavage of Thiazole-2 Derivatives Under Acidic Conditions. *Tetrahedron* **2010**, *66*, 8661–8666.
- Michalska, J.; Boduszek, B.; Olszewski, T. K. New Quinoline-2, -3, and 4-yl-(amino) Methylphosphonates: Synthesis and Study on the C-P Bond Cleavage in Quinoline-2 and -4 Derivatives Under Acidic Conditions. *Heteroatom Chem.* **2011**, *22*, 617–624.
- Kirk, R. E.; Othmer, D. F. *Kirk-Othmer Encyclopedia of Chemical Technology*; John Wiley & Sons: New York, 2005.

- (9) Mucha, A.; Kafarski, P.; Berlicki, Ł. Remarkable Potential of the  $\alpha$ -Aminophosphonate/Phosphinate Structural Motif in Medicinal Chemistry. *J. Med. Chem.* **2011**, *54*, 5955–5980.
- (10) Kudzin, Z. H.; Gralak, D. K.; Andrijewski, G.; Drabowicz, J.; Luczak, J. Simultaneous Analysis of Biologically Active Amino-alkanephosphonic Acids. *J. Chromatogr. A* **2003**, *998*, 183–199.
- (11) Gilbert, S. G. *A Small Dose of Toxicology: The Health Effects of Common Chemicals*; CRC Press: New York, 2005.
- (12) Olszewski, T. K.; Boduszek, B.; Sobek, S.; Kozłowski, H. Synthesis of Thiazole Aminophosphine Oxides, Aminophosphonic and Aminophosphinic Acids and Cu(II) Binding Abilities of Thiazole Aminophosphonic Acids. *Tetrahedron* **2006**, *62*, 2183–2189.
- (13) Kafarski, P.; Lejczak, B. Application of Bacteria and Fungi as Biocatalysts for the Preparation of Optically Active Hydroxyphosphonates. *J. Mol. Catal. B-Enzym.* **2004**, *29*, 99–104.
- (14) Kafarski, P.; Lejczak, B.; Tyka, R.; Koba, L.; Pliszczak, E.; Wieczorek, P. Herbicidal Activity of Phosphonic, Phosphinic, and Phosphonous Acid Analogues of Phenylglycine and Phenylalanine. *J. Plant Growth Regul.* **1995**, *14*, 199–203.
- (15) Mucha, A.; Tyka, R.; Kafarski, P.; Głowiak, T.; Goplańska, A. Preparation, Crystal and Molecular Structure, and Evaluation of Plant Growth Regulating Activity of Guanidinoalkanephosphinates and Phosphonates. *Heteroatom Chem.* **1995**, *6*, 433–441.
- (16) Podstawka-Proniewicz, E.; Andrzejak, M.; Kafarski, P.; Kim, Y.; Proniewicz, L. M. Vibrational Characterization of L -Valine Phosphonate Dipeptides: FT-IR, FT-RS, and SERS Spectroscopy Studies and DFT Calculations. *J. Raman Spectrosc.* **2011**, *42*, 958–979.
- (17) Podstawka, E.; Kudelski, A.; Olszewski, T. K.; Boduszek, B. Surface-Enhanced Raman Scattering Studies on the Interaction of Phosphonate Derivatives of Imidazole, Thiazole, and Pyridine with a Silver Electrode in Aqueous Solution. *J. Phys. Chem. B* **2009**, *113*, 10035–10042.
- (18) Podstawka, E.; Ozaki, Y. Surface-Enhanced Raman Difference Between Bombesin and Its Modified Analogs on the Colloidal and Electrochemically Roughen Silver Surfaces. *Biopolymers* **2008**, *89*, 807–819.
- (19) Podstawka-Proniewicz, E.; Ozaki, Y.; Kim, Y.; Xu, Y.; Proniewicz, L. M. Surface-Enhanced Raman Scattering Studies on Bombesin, Its Selected Fragments and Related Peptides Adsorbed at the Silver Colloidal Surface. *Appl. Surf. Sci.* **2011**, *257*, 8246–8252.
- (20) Podstawka, E.; Kafarski, P.; Proniewicz, L. M. Effect of an Aliphatic Spacer Group on the Adsorption Mechanism on the Colloidal Silver Surface of L-Proline Phosphonodipeptides. *J. Raman Spectrosc.* **2008**, *39*, 1726–1739.
- (21) Podstawka, E.; Andrzejak, M.; Kafarski, P.; Proniewicz, L. M. Comparison of Adsorption Mechanism on Colloidal Silver Surface of Alafosfalin and Its Analogs. *J. Raman Spectrosc.* **2008**, *39*, 1238–1249.
- (22) Piergies, N.; Proniewicz, E.; Kudelski, A.; Rydzewska, A.; Kim, Y.; Andrzejak, M.; Proniewicz, L. M. Fourier Transform Infrared and Raman and Surface-Enhanced Raman Spectroscopy Studies of a Novel Group of Boron Analogues of Aminophosphonic Acids. *J. Phys. Chem. A* **2012**, *116*, 10004–10014.
- (23) Proniewicz, E.; Piergies, N.; Ozaki, Y.; Kim, Y.; Proniewicz, L. M. Investigation of Adsorption Mode of a Novel Group of N-Benzylamino(boronphenyl)methylphosphonic Acids Using SERS. *Spectrochim. Acta, Part A* **2013**, *103*, 167–172.
- (24) Lee, P. C.; Meisel, D. Adsorption and Surface-Enhanced Raman of Dyes on Silver and Gold Sols. *J. Phys. Chem.* **1982**, *86*, 3391–3395.
- (25) Kneipp, K.; Kneipp, H.; Itzkan, I.; Dasari, R. R.; Feld, M. S. Surface-Enhanced Raman Scattering and Bophysics. *J. Phys.: Condens. Matter* **2002**, *14*, R597–R624.
- (26) Birke, R. L.; Znamenskiy, V.; Lombardi, J. R. A Charge-Transfer Surface Enhanced Raman Scattering Model from Time-Dependent Density Functional Theory Calculations on a Ag10 -Pyridine Complex. *J. Chem. Phys.* **2010**, *132*, 214707-1–214707-15.
- (27) Moskovits, M. Surface Selection Rules. *J. Chem. Phys.* **1982**, *77*, 4408–4416.
- (28) Moskovits, M. Surface-Enhanced Spectroscopy. *Rev. Mod. Phys.* **1985**, *57*, 783–826.
- (29) Gao, X.; Davies, J. P.; Weaver, M. J. Test of Surface Selection Rules for Surface-Enhanced Raman Scattering: The Orientation of Adsorbed Benzene and Monosubstituted Benzenes on Gold. *J. Phys. Chem.* **1990**, *94*, 6858–6864.
- (30) Goldeman, W.; Boduszek, B. Aminophosphinic Acids in a Pyridine Series, Part 2: Synthesis of 2-, 3-, and 4-Pyridyl Derivatives of 1-(Benzylamino)-methyl-H-phosphinic Acids. *Phosphorus Sulfur* **2009**, *184*, 1413–1425.
- (31) Podstawka, E.; Ozaki, Y.; Proniewicz, L. M. Structures and Bonding on a Colloidal Silver Surface of the Various Length Carboxyl Terminal Fragments of Bombesin. *Langmuir* **2008**, *24*, 10807–10816.
- (32) Pięta, E.; Proniewicz, E.; Kim, Y.; Proniewicz, L. M. Vibrational Characterization and Adsorption Mode on SERS-Active Surfaces of Guanidino-(bromophenyl)methylphosphonic Acid. *Spectrochim. Acta A* **2014**, *121*, 121–128.
- (33) Moskovits, M.; DiLella, D. P.; Maynard, K. J. Surface Raman Spectroscopy of a Number of Cyclic and Molecular Reorientation Aromatic Molecules Adsorbed on Silver: Selection Rules. *Langmuir* **1988**, *4*, 67–76.
- (34) Nakanishi, K.; Sakiyama, T.; Imamura, K. On the Adsorption of Proteins on Solid Surfaces, a Common but Very Complicated Phenomenon. *J. Biosci. Bioeng.* **2001**, *91*, 233–244.
- (35) Creighton, J. A. Surface Raman Electromagnetic Enhancement Factors For Molecules at the Surface of Small Isolated Metal Spheres: the Determination of Adsorbate Orientation from SERS Relative Intensities. *Surf. Sci.* **1983**, *124*, 209–219.
- (36) Podstawka, E.; Kudelski, A.; Proniewicz, L. M. Adsorption Mechanism of Physiologically Active L-Phenylalanine Phosphonodipeptide Analogs: Comparison of Colloidal Silver and Macroscopic Silver Substrates. *Surf. Sci.* **2007**, *601*, 4971–4983.
- (37) Podstawka, E.; Kudelski, A.; Kafarski, P.; Proniewicz, L. M. Influence of Aliphatic Spacer Group on Adsorption Mechanisms of Phosphonate Derivatives of L-Phenylalanine: Surface-Enhanced Raman, Raman, and Infrared Studies. *Surf. Sci.* **2007**, *601*, 4586–4597.
- (38) Castro, J. L.; López Ramírez, M. R.; López Tocón, I.; Otero, J. C. Vibrational Study of the Metal-Adsorbate Interaction of Phenylacetic Acid and  $\alpha$ -Phenylglycine on Silver Surfaces. *J. Colloid Interface Sci.* **2003**, *263*, 357–363.
- (39) Carter, D. A.; Pemberton, J. E. Surface-Enhanced Raman Scattering of the Acid-Base Forms of Imidazole on Ag. *Langmuir* **1992**, *8*, 1218–1225.
- (40) Podstawka, E.; Kudelski, A.; Drag, M.; Oleksyszyn, J.; Proniewicz, L. M. Adsorbed States of Substituted  $\alpha$ -Aminophosphinic Acids on a Silver Electrode Surface: Comparison with a Colloidal Silver Substrate. *J. Raman Spectrosc.* **2009**, *40*, 1578–1584.
- (41) Podstawka-Proniewicz, E.; Kudelski, A.; Kim, Y.; Proniewicz, L. M. Structure and Binding of Specifically Mutated Neurotensin Fragments on a Silver Substrate: Vibrational Studies. *J. Phys. Chem. B* **2011**, *115*, 7097–7108.
- (42) Proniewicz, E.; Pięta, E.; Kudelski, A.; Piergies, N.; Skoluba, D.; Kim, Y.; Proniewicz, L. M. Vibrational and Theoretical Studies of the Structure and Adsorption Mode of m-Nitrophenyl  $\alpha$ -Guanidinomethylphosphonic Acid Analogues on Silver Surfaces. *J. Phys. Chem. A* **2013**, *117*, 4963–4972.
- (43) Frisch, M. J.; Trucks, G. W.; Schlegel, H. B.; Scuseria, G. E.; Robb, M. A.; Cheeseman, J. R.; Montgomery, J. A.; Vreven, T.; Kudin, K. N.; Burant, J. C.; et al. *Gaussian03*, Revision A.1; Gaussian Inc.: Pittsburgh, PA, 2003.
- (44) Jensen, F. *Introduction to Computational Chemistry*; John Wiley and Sons Ltd: Chichester, U.K., 2007.
- (45) Frisch, M. J.; Pople, J. A.; Binkley, J. S. Self-Consistent Molecular Orbital Methods 25. Supplementary Functions for Gaussian Basis Sets. *J. Chem. Phys.* **1984**, *80*, 3265–3269.
- (46) Michalska, D.; Wysokiński, R. The Prediction of Raman Spectra of Platinum(II) Anticancer Drugs by Density Functional Theory. *Chem. Phys. Lett.* **2005**, *403*, 211–217.
- (47) O’Boyle, N. M.; Vos, J. G. *GaussSum 0.8*; Dublin City University: Dublin, 2004. Available at <http://gausssum.sourceforge.net>.

- (48) Martin, J. L. M.; Van Alsenoy, C. *Gar2ped*; University of Antwerp: Antwerp, 1995.
- (49) Steiner, T. The Hydrogen Bond in the Solid State. *Angew. Chem., Int. Ed.* **2002**, *41*, 48–76.
- (50) Wu, D.-Y.; Ren, B.; Jiang, Y.-X.; Xu, X.; Tian, Z.-Q. Density Functional Study and Normal-Mode Analysis of the Bindings and Vibrational Frequency Shifts of the Pyridine-M ( $M = Cu, Ag, Au, Cu^+, Ag^+, Au^+$ , and Pt) Complexes. *J. Phys. Chem. A* **2002**, *106*, 9042–9052.
- (51) Kiefer, J. H.; Zhang, Q.; Kern, R. D.; Yao, J.; Jursic, B. Pyrolyses of Aromatic Azines: Pyrazine, Pyrimidine, and Pyridine. *J. Phys. Chem. A* **1997**, *101*, 7061–7073.
- (52) Hilliard, C. R.; Bhuvanesh, N.; Gladysz, J. A.; Blümel, J. Synthesis, Purification, and Characterization of Phosphine Oxides and Their Hydrogen Peroxide Adducts. *Dalton Trans.* **2012**, *41*, 1742–1754.
- (53) Kalenius, E.; Neitola, R.; Suman, M.; Dalcanale, E.; Vainiotalo, P. Hydrogen Bonding in Phosphonate Cavitands: Investigation of Host–Guest Complexes with Ammonium Salts. *J. Am. Soc. Mass Spectrom.* **2010**, *21*, 440–450.
- (54) Eker, F.; Cao, X.; Nafie, L.; Schweitzer-Stenner, R. Tripeptides Adopt Stable Structures in Water. A Combined Polarized Visible Raman, FTIR, and VCD Spectroscopy Study. *J. Am. Chem. Soc.* **2002**, *124*, 14330–14341.
- (55) Sett, P.; Chattopadhyay, S.; Mallick, P. K. Raman Excitation Profiles and Excited State Molecular Configurations of Three Isomeric Phenyl Pyridines. *Spectrochim. Acta, Part A* **2000**, *56*, 855–875.
- (56) Buntinx, G.; Naskrecki, R.; Didierjean, C.; Poizat, O. Transient Absorption and Time-Resolved Raman Study of the Photophysics of 4-Phenylpyridine in Solution. *J. Phys. Chem. A* **1997**, *101*, 8768–8777.
- (57) Testa, A. C.; Schneider, S.; Brem, B. Time-Resolved Resonance Raman Study of 4-Phenylpyridine. *J. Photochem. Photobiol. A* **1997**, *107*, 147–152.
- (58) López Tocón, I.; Woolley, M. S.; Otero, J. C.; Marcos, J. I. Vibrational Spectrum of 3-Methyl and 4-Methylpyridine. *J. Mol. Struct.* **1998**, *470*, 241–246.
- (59) Wysokiński, R.; Michalska, D.; Bieńko, D. C.; Ilakiamani, S.; Sundaraganesan, N.; Ramalingam, K. Density Functional Study on the Molecular Structure, Infrared and Raman Spectra, and Vibrational Assignment for 4-Thiocarbamoylpyridine. *J. Mol. Struct.* **2006**, *791*, 70–76.
- (60) Dressler, D. H.; Mastai, Y.; Rosenbluh, M.; Fleger, Y. Surface-Enhanced Raman Spectroscopy as a Probe for Orientation of Pyridine Compounds on Colloidal Surfaces. *J. Mol. Struct.* **2009**, *935*, 92–96.
- (61) Wen, R.; Fang, Y. Adsorption of Pyridine Carboxylic Acids on Silver Surface Investigated by Potential-Dependent SERS. *Vibr. Spectrosc.* **2005**, *39*, 106–113.
- (62) Gao, P.; Weaver, M. J. Surface-Enhanced Raman Spectroscopy as a Probe of Adsorbate-Surface Bonding: Benzene and Monosubstituted Benzenes Adsorbed at Gold Electrodes. *J. Phys. Chem.* **1985**, *89*, 5040–5046.
- (63) Podstawska, E.; Borszowska, R.; Grabowska, M.; Drag, M.; Kafarski, P.; Proniewicz, L. M. Investigation of Molecular Structures and Adsorption Mechanisms of Phosphonodipeptides by Surface-Enhanced Raman, Raman, and Infrared Spectroscopies. *Surf. Sci.* **2005**, *599*, 207–220.
- (64) Durrell, A. C.; Gray, H. B.; Hazari, N.; Incarvito, C. D.; Liu, J.; Yan, E. C. Y. Tris(hydroxypropyl)phosphine Oxide: A Chiral Three-Dimensional Material with Nonlinear Optical Properties. *Cryst. Growth Des.* **2010**, *10*, 1482–1485.
- (65) Wilson, E. B., Jr. The Normal Modes and Frequencies of Vibration of the Regular Plane Hexagon Model of the Benzene Molecule. *Phys. Rev.* **1934**, *45*, 706–714.
- (66) Klots, T. D. Raman Vapor Spectrum and Vibrational Assignment for Pyridine. *Spectrochim. Acta Part A* **1998**, *54*, 1581–1488.
- (67) Centeno, S. P.; López-Tocón, I.; Arenas, J. F.; Soto, J.; Otero, J. C. Selection Rules of the Charge Transfer Mechanism of Surface-Enhanced Raman Scattering: The Effect of the Adsorption on the Relative Intensities of Pyrimidine Bonded to Silver Nanoclusters. *J. Phys. Chem. B* **2006**, *110*, 14916–14922.
- (68) Arenas, J. F.; Tocón, I. L.; Otero, J. C.; Marcos, J. I. Charge Transfer Processes in Surface-Enhanced Raman Scattering. Franck-Condon Active Vibrations of Pyridine. *J. Phys. Chem.* **1996**, *100*, 9254–9261.
- (69) Lombardi, J. R.; Birke, R. L. A Unified View of Surface-Enhanced Raman Scattering. *Acc. Chem. Res.* **2009**, *42*, 734–742.